Alteration of long and short-term hematopoietic stem cell ratio causes myeloid-biased hematopoiesis

Running title; Self-renewal heterogeneity causes myeloid skewing

Katsuyuki Nishi[1,2], Taro Sakamaki[1,2], Akiomi Nagasaka[1,2], Kevin S. Kao[3], Kay Sadaoka[1,2], Masahide Asano[4], Nobuyuki Yamamoto[5], Akifumi Takaori-Kondo[6], Masanori Miyanishi[1,2] *

[1]Hematopoietic Stem Cell Biology and Medical Innovation (HSCBMI), Department of Pediatrics, Kobe University Graduate School of Medicine, Kobe, Hyogo 650-0047, Japan

[2]RIKEN Center for Biosystems Dynamics Research, Kobe, Hyogo 650-0047, Japan

[3]Weill Cornell, Rockefeller, Sloan-Kettering, Tri-Institutional MD-PhD Program, New York, NY

[4]Institute of Laboratory Animals, Kyoto University Graduate School of Medicine, Kyoto, Kyoto, 606-8501, Japan.

[5]Department of Pediatrics, Kobe University Graduate School of Medicine, Kobe, Hyogo 650-0017, Japan

[6]Department of Hematology and Oncology, Kyoto University Graduate School of Medicine, Kyoto, Kyoto 606-8507, Japan

*Correspondence: Masanori Miyanishi, M.D, Ph.D.

Hematopoietic Stem Cell Biology and Medical Innovation (HSCBMI), Department of Pediatrics, Kobe University Graduate School of Medicine, Kobe, Hyogo 650-0047, Japan

E-mail: miya75@med.kobe-u.ac.jp

Phone: 078-304-6037

FAX: 078-304-6100

Abstract

Myeloid-biased hematopoiesis is a well-known age-related alteration. Several possibilities, including myeloid-biased hematopoietic stem cell (HSC) clones, may explain this. However, the precise mechanisms remain controversial.

Utilizing the Hoxb5 reporter system to prospectively isolate long-term HSCs (LT-HSCs) and short-term HSCs (ST-HSCs), we found that young and aged LT-HSCs co-transplanted into the same recipients demonstrated nearly equivalent myeloid lineage output, contrary to the theory of myeloid-biased HSC clones. Transcriptomics indicated no significant myeloid gene enrichment in aged LT-HSCs compared to their young counterparts. Instead, transplanting reconstituted young HSCs with the ratio of LT/ST-HSCs seen in aged mice can significantly skew the lineage output to myeloid cells. In addition, while the niche environment in the bone marrow minimally affects myeloid-biased hematopoiesis, aged thymi and spleens substantially hinder lymphoid hematopoiesis, resulting in further myeloid-domination. Thus, we demonstrate that myeloid-biased hematopoiesis in aged organisms originates due to alteration of the ratio between LT-HSCs and ST-HSCs rather than in heterogeneous HSC clones with various cell fates.

Introduction

Age-associated changes in individuals are deeply correlated with progressive attenuation of cellular functions in tissue stem cells of organs (Jones and Rando 2011). In the hematopoietic system, hematopoietic stem cells (HSCs), which possess self-renewal capacity and multipotency (Spangrude et al., 1988; Weissman and Shizuru 2008; Majeti et al., 2007), are responsible for various hematopoietic alterations with age, such as reduced self-renewal capacity (Morrison et al., 1996) and myeloid-biased hematopoiesis (Muller-Sieburg et al., 2004; Challen et al., 2010) due to their functional decline. For example, myeloid-biased hematopoiesis potentially reduces response to infections (Webster, 2000), reduces vaccination efficacy (Crooke et al., 2019), and increases myeloid malignancy (Rossi et al., 2008) in aged individuals. To comprehend these age-associated physiological changes, myeloid-biased hematopoiesis has been studied in considerable detail.

Based on the experimental observation that transplantation of aged HSCs exhibits more myeloid-biased differentiation in young recipient mice than transplantation of young HSCs, this phenotype has been thought to originate in cell-intrinsic changes in the HSC compartment (Geiger et al., 2013; De Haan and Lazare 2018; Schultz and Sinclair 2016). A myeloid-biased phenotype after aged HSC transplantation leads to the suggestion that myeloid-biased HSC clones selectively expand with age (Cho et al., 2008; Pang et al., 2011). Transcriptome and epigenetic analyses showing that a set of genes related to myeloid differentiation is significantly enriched in aged HSCs compared to young HSCs (Rossi et al., 2005; Grover et al., 2016) further supports this hypothesis.

On the other hand, some reports support a different point of view in light of experimental evidence showing that aged lymphoid-biased HSCs still demonstrate the same level of

89 lymphopoiesis as their younger counterparts, despite exhibiting a myeloid-biased gene
90 expression pattern (Montecino-Rodriguez et al., 2019). This result highlights the
91 limitations of predicting a pattern of HSC differentiation based upon gene expression
92 patterns. Moreover, myeloid progenitors such as granulocyte-macrophage progenitor
93 (GMP) and common myeloid progenitor (CMP) should also increase with age if the
94 selective expansion of myeloid-biased HSCs leads to an increase of myeloid cells in
95 peripheral blood (PB). However, increment of such progenitors with age was not
96 consistently demonstrated in earlier research (Rossi et al., 2005; Nilsson et al., 2016; Min
97 et al., 2006). Additionally, a mathematical model demonstrated that aging had no effect
98 on the daily production of CMP supplied from multipotent progenitors (MPP) (Busch et
99 al., 2015; Dorshkind et al., 2020).
100 As such, while selective expansion of myeloid-biased HSC clones is the most widely
101 accepted hypothesis to explain myeloid-biased hematopoiesis in aging (Mejia-Ramirez
102 and Florian, 2020; SanMiguel et al., 2020), other mechanisms may exist in light of the
103 inconsistent cellular behavior of progenitor fractions relative to HSCs. To the best of our
104 knowledge, no reports have analyzed kinetics of age-associated changes in HSCs,
105 progenitors, and PB cells simultaneously. Therefore, we started our investigation by
106 examining the correlation between age-related changes in PB and BM to shed light on
107 the mechanism underlying myeloid-biased hematopoiesis that occurs during aging.
108
109 **Results**
110 ***The discrepancy of age-associated alternation in peripheral blood and bone marrow***
111 ***calls into question the existence of a myeloid-biased clone***

112 Mouse HSC research on aging has used mice aged 18 months or older (Challen et al.,
113 2010; Cho et al., 2008; D. J. Rossi et al., 2005; Grover et al., 2016; Montecino-Rodriguez
114 et al., 2019; Nilsson et al., 2016). However, given that continuous accumulation of
115 cellular stress with age causes a gradual decline of cellular functions, a comprehensive
116 analysis from young to old mice is necessary to unravel mechanisms by which age-
117 associated, myeloid-biased hematopoiesis progress. Hence, we analyzed changes in PB
118 (**Fig. S1 A**) at multiple time points from young to old mice. These results showed that the
119 percentage of myeloid cells began to change as early as 6 months in mice and continued
120 to increase at a constant rate until the age of ≥ 23 months (**Fig. 1 A**).

121 It has been reported that myeloid-biased hematopoiesis is caused by a selective increase
122 of myeloid-biased clones in the immunophenotypically defined (surface-antigen
123 defined) HSC fraction (**Fig. S1 B**) (Beerman et al., 2010). According to this hypothesis,
124 age-associated myeloid hematopoiesis progression in PB would be paralleled by an
125 increase in myeloid-biased HSC clones. Therefore, we examined the frequency of the
126 HSC and progenitor fractions in the BM at multiple time points (**Fig. S1, B and C**). We
127 found that the frequency of immunophenotypically defined HSC in BM rapidly increased
128 up to the age of 12 months. After the age, they remained plateaued throughout the
129 observation period (**Fig. 1 B**). On the other hand, in contrast to what we anticipated, the
130 frequency of GMP was stable, and the percentage of CMP actually decreased
131 significantly with age, defying our prediction that the frequency of components of the
132 myeloid differentiation pathway, such as CMP, GMP, and MEP would increase in aged
133 mice if myeloid-biased HSC clones increase with age (**Fig. 1 B**).

134 Finally, we determined the ratio of each fraction in young mice versus aged mice to
135 compare the age-associated transition pattern of components comprising the myeloid

136 differentiation pathway. This analysis revealed that age-associated transition patterns of
137 immunophenotypically defined HSC and CMP in BM were not paralleled with myeloid
138 cell in PB (**Fig. 1 C**). These findings called into question the hypothesis that there is a
139 selective increase of myeloid-biased HSC clones in the aged BM. We then set out to
140 elucidate the mechanism by which myeloid-biased phenotypes arise in the PB of aged
141 mice.
142
143 ***The long-term observation of 2-year-old LT-HSC's differentiation does not indicate the***
144 ***expansion of myeloid-biased clones.***
145 Numerous studies have claimed that the myeloid-skewed phenotype observed in PB of
146 aged mice is caused by myeloid-biased HSC clones selectively expanded from HSCs with
147 originally heterogeneous differentiation potentials (Beerman et al., 2010; Dykstra et al.,
148 2011; Sudo et al., 2000). Other studies have reported that immunophenotypically defined
149 HSCs possess heterogeneity associated with self-renewal capacity, suggesting the
150 existence of at least two different populations in the HSC compartment, LT-HSCs and
151 ST-HSCs (Morrison and Weissman 1994; Spangrude et al., 1995). Since LT-HSCs have
152 extensive self-renewal capacity, while ST-HSCs lose their self-renewal capacity within a
153 short period, LT-HSCs are thought to persist in the BM throughout life and to enrich age-
154 associated changes compared to ST-HSCs. Therefore, we expect that LT-HSC-specific
155 analyses will help to answer whether myeloid-biased HSC clones exist.
156 We previously reported that Hoxb5 exclusively marks LT-HSCs in young mice (Chen et
157 al., 2016). However, we have not tested in aged mice whether Hoxb5 specifically labels
158 LT-HSCs and helps to distinguish LT-HSCs and ST-HSCs from immunophenotypically
159 defined HSCs (hereafter, bulk-HSCs). To confirm this, we first analyzed expression of

160 Hoxb5 in bulk-HSC, MPP, Flk2^{+}, and Lin^{-}Sca1^{-}c-Kit^{+} populations in aged *Hoxb5*-tri-
161 mCherry mice. We observed that Hoxb5 was exclusively expressed in bulk-HSCs (**Fig.**
162 **2 A**). Then, to verify long-term engraftment, we conducted a transplantation assay
163 utilizing Hoxb5^{+} HSCs and Hoxb5^{-} HSCs, respectively, isolated from 2-year-old mice
164 (**Fig. 2 B**). We observed that only recipients receiving aged Hoxb5^{+} HSCs exhibited
165 continuous hematopoiesis 16 weeks after primary transplantation (**Fig. 2, C and E; Fig.**
166 **S2 A**). In secondary transplantation analysis, only recipients receiving Hoxb5^{+} HSCs
167 exhibited robust hematopoiesis throughout the period of observation, indicating that
168 Hoxb5 can be used as a specific marker of LT-HSCs in aged mice, as well as young mice
169 (**Fig. 2, D and F; Fig. S2 B**).
170 A serial transplantation assay with a period of observation longer than 8 months should
171 be long enough to observe further myeloid-biased change. If bulk-HSCs isolated from
172 aged mice are already enriched by myeloid-biased HSC clones, we should see more
173 myeloid-biased phenotypes 16 weeks after primary and the secondary transplantation.
174 However, we found that kinetics of the proportion of myeloid cells in PB were similar
175 across primary and the secondary transplantation and that the proportion of myeloid cells
176 gradually decreased over time (**Fig. 2 G**). These results suggest the following two
177 possibilities: either myeloid-biased HSCs do not expand in the LT-HSC fraction, or the
178 expansion of myeloid-biased clones in 2-year-old mice has already peaked.
179
180 ***Direct comparison between young vs. aged LT-HSC differentiation reveals that LT-***
181 ***HSCs exhibit unchanged lineage output throughout life***
182 We developed a co-transplantation assay to directly compare the differentiation capacity
183 between young and aged LT-HSCs by co-transplanting ten young GFP^{+} LT-HSCs and

184 ten aged GFP$^-$ LT-HSCs into the same recipient mice (**Fig. 3 A**). Then, we found that the
185 myeloid lineage proportions from young and aged LT-HSCs were nearly comparable
186 during the observation period after transplantation (**Fig. 3, B and C**). Furthermore, by
187 analyzing the proportion of mature cell types derived from young and aged LT-HSCs in
188 the same donor, we directly compared the capacity for hematopoietic reconstitution in
189 each mature cell type between young and aged LT-HSCs. We confirmed again that the
190 reconstitution ratio was almost the same across all lineages, although bulk hematopoiesis
191 derived from young LT-HSCs predominated (**Fig. 3 D**). These results indicate that the
192 differentiation potential of LT-HSCs remains unchanged throughout their lives.
193 Several reports have demonstrated that transplanting mixed/bulk-HSCs—a combination
194 of LT-HSCs and ST-HSCs—obtained from old animals results in blatantly myeloid-
195 biased hematopoiesis (Beerman et al., 2010; Dykstra et al., 2011; Sudo et al., 2000). To
196 test this, we co-transplanted bulk-HSCs from young and old mice to corroborate this (**Fig.
197 S3 A**). As previously described, we observed that aged bulk-HSC exhibited a myeloid-
198 skewed phenotype (**Fig. S3 B and C**). Additionally, we observed that aged bulk-HSC
199 reconstitution exhibited higher reconstitution of myeloid cells compared to young bulk-
200 HSCs (**Fig. S3 D**). These findings unmistakably demonstrated that mixed/bulk-HSCs
201 showed myeloid skewed hematopoiesis in PB with aging, while LT-HSCs exhibited
202 unchanged lineage output throughout life.
203
204 ***LT-HSCs never show myeloid-related gene set enrichment during aging***
205 Although the results of co-transplantation of young and aged LT-HSCs did not
206 demonstrate lineage-biased output by LT-HSCs throughout life, enrichment of myeloid
207 genes in aged bulk-HSCs shown by previous studies supports the idea that myeloid-

208 biased hematopoiesis is caused by selective expansion of myeloid-biased HSC clones (D.
209 J. Rossi et al., 2005; Grover et al., 2016). To compare age-associated myeloid gene
210 enrichment, we isolated bulk-HSC, LT-HSCs, and ST-HSCs from young or aged mice
211 (**Fig. 4 A**).
212 To ensure the quality of the sorted fraction for subsequent RNA-seq analyses, we verified
213 the Hoxb5 read counts (**Fig. S4 A**). Cluster dendrograms using the whole transcriptome
214 confirmed that cell fractions isolated from young and aged mice clustered into distinct
215 groups (**Fig. 4 B**). Then, using sets of aging-related genes, such as inflammation
216 (Liberzon et al., 2015; Pietras 2017), DNA damage (p53 pathway) (Liberzon et al., 2015;
217 D. J. Rossi et al., 2007), cell cycle progression (E2F target) (Liberzon et al., 2015;
218 Kowalczyk et al., 2015), and a common aging signature (Flohr Svendsen et al., 2021), we
219 ran a violin plot analysis on each cell fraction to confirm the occurrence of typical aging-
220 related gene expression changes. We found age-associated changes in inflammation and
221 the DNA damage between cells isolated from young and aged mice, but very similar
222 patterns regardless of cell fraction in young or aged mice. In terms of cell cycle
223 progression and aging signature genes, however, we discovered that only the young LT-
224 HSC fraction differed from other young fractions and tended to represent similar gene
225 expression pattern with aged fractions (**Fig. 4 C**). Then, taking LT-HSC specific gene
226 expression pattern into account, we looked at expression patterns of specific genes that
227 had been highly validated by experiments as being associated with myeloid-biased HSC
228 (Beerman et al., 2010; Flohr Svendsen et al., 2021; Sanjuan-Pla et al., 2013; Mann et al.,
229 2018). We discovered that expression of these genes is relatively comparable between
230 young and aged LT-HSCs, but not other fractions (**Fig. S4 B**).

231 A recent comprehensive analysis of mouse HSC aging using multiple RNAseq data sets
232 claimed that almost 80% of differentially expressed genes are poorly reproducible across
233 data sets (Flohr Svendsen et al., 2021). In fact, we found that almost 80% of genes are
234 not shared when we compare three representative myeloid/lymphoid gene sets (Sanjuan-
235 Pla et al., 2013; Chambers et al., 2007; Pronk et al., 2007). Additionally, most genes were
236 only used in a single gene set (**Fig. 4, D and E**). By using only genes that were shared in
237 these gene sets, we ran a gene set enrichment analysis (GSEA) to see whether
238 myeloid/lymphoid genes were enriched in aged LT-HSCs or other fractions. Neither aged
239 LT-HSC nor aged ST-HSC exhibited myeloid/lymphoid gene enrichment, while shared
240 myeloid-related genes tended to be enriched in aged bulk-HSCs (**Fig. 4, F and G**). On
241 the other hand, GSEA analysis using original gene sets, respectively, showed inconsistent
242 results (**Fig. S4, C and D**).
243
244 ***A myeloid-biased phenotype in peripheral blood depends on the relative decrease of***
245 ***ST-HSC in the HSC compartment with age***
246 While transplantation of aged bulk-HSCs exhibits a myeloid-biased phenotype in PB
247 shown in previous reports (Beerman et al., 2010; Dykstra et al., 2011; Sudo et al., 2000)
248 and our results (**Fig. S3**), aged LT-HSCs remain stable in terms of the balance of their
249 differentiation potential between myeloid and lymphoid production (**Fig. 3**). Comparative
250 transcriptome analyses demonstrated that neither LT-HSCs nor ST-HSCs, which are
251 functionally more homogeneous than bulk-HSCs, exhibited myeloid gene set enrichment
252 with age, whereas aged bulk-HSCs tended to show more myeloid gene set enrichment
253 than their young counterparts (**Fig. 4**). We then tried to figure out what causes the
254 myeloid-biased phenotype in PB after transplantation of bulk-HSCs.

255 Because LT-HSCs in bulk-HSCs exhibit nearly constant level of hematopoiesis
256 throughout life, we hypothesized that ST-HSCs could be the key to discovering
257 mechanisms underlying the myeloid-skewing phenomenon. First, we revisited our
258 previous study (Chen et al., 2016), which demonstrated that transplanted ST-HSCs
259 maintain lymphocyte production while rapidly losing myeloid lineage production in
260 recipients. This result may potentially indicate the presence of HSC clones with a
261 preference for lymphoid differentiation. Given that donor cells obtained from primary
262 recipients receiving ST-HSCs do not undergo hematopoiesis in secondary transplantation
263 (Chen et al., 2016), it is likely that all ST-HSCs have already lost their ability to self-
264 renew and have disappeared from the HSC fraction in primary recipients. To confirm this,
265 we transplanted ten LT-HSCs or ST-HSCs and then analyzed PB and BM (**Fig. 5 A**). As
266 we previously reported (Chen et al., 2016), donor-derived hematopoiesis eventually
267 becomes lymphocyte-dominant in PB of ST-HSC recipients over time (**Fig. 5 B**).
268 Subsequently, it was determined that the vast majority of T cell subsets are memory cells
269 (**Fig. 5, C and D**). In addition, unlike recipients receiving LT-HSCs, recipients receiving
270 ST-HSCs lacked any bulk-HSCs in their BM (**Fig. 5, E and F**). These results strongly
271 suggest that lymphoid-biased hematopoiesis observed after transplantation of ST-HSCs
272 is due to persistence of memory-type lymphocytes in PB, rather than to *de novo*
273 lymphopoiesis from lymphoid-biased HSC clones. Persistence of memory-type
274 lymphocytes from ST-HSCs may have led us to misinterpret mechanisms underlying
275 myeloid-biased hematopoiesis after aged bulk-HSC transplantation. To verify this
276 hypothesis, we examined kinetics of the LT-HSC/ST-HSC ratio in the bulk-HSC
277 population, revealing the ratio of ST-HSC to LT-HSC decreased with age (**Figure S5**).

278 Thus, we hypothesized that the relative decrease in the ST-HSC ratio in the aged bulk-
279 HSC fraction would lead to reduction of memory-type lymphocytes and myeloid-biased
280 hematopoiesis following transplantation of aged bulk-HSCs. To test this hypothesis, we
281 isolated LT-HSCs and ST-HSCs from young donor mice and reconstituted them with a
282 2:8 ratio (as in young mice) or a 5:5 ratio (as in aged mice) prior to transplanting them
283 (**Fig. 6 A**). Four weeks after transplantation, PB analysis revealed that both groups had
284 comparable patterns of hematopoiesis. In contrast, recipient mice transplanted with a 5:5
285 ratio began to exhibit more myeloid-biased hematopoiesis eight weeks after
286 transplantation, and by week 16, they produced significantly more myeloid cells than the
287 other group (**Fig. 6, B-D**). Additionally, we conducted further investigations to determine
288 whether lymphoid hematopoiesis could be accelerated by alteration of LT-HSC/ST-HSC
289 ratios using cells from aged mice. To verify this, we isolated aged LT-HSCs and ST-
290 HSCs and reconstituted them with a 5:5 ratio or a 2:8 ratio prior to transplantation (**Fig.
291 S6 A**). Peripheral blood analysis revealed that lymphoid lineage output in the recipient
292 mice transplanted with a 2:8 ratio was significantly greater than those with a 5:5 ratio
293 (**Fig. S6 B-D**). Based on these findings, we concluded that myeloid-biased hematopoiesis
294 observed following transplantation of aged HSCs was caused by a relative decrease in
295 ST-HSC in the bulk-HSC compartment in aged mice rather than the selective expansion
296 of myeloid-biased HSC clones.
297
298 ***Age-associated extramedullary changes accelerate myeloid-biased hematopoiesis***
299 We found that the fluctuating LT-HSC/ST-HSC ratio in the bulk-HSC compartment
300 corresponded with the myeloid-biased hematopoiesis associated with aging. In contrast,
301 the degree of myeloid bias observed in mice older than 23 months without transplantation

302 (**Fig. 1 A**; 49.0 ± 23.4%) was significantly greater than in recipient mice receiving young
303 mixed HSCs with a 5:5 ratio 16 weeks after transplantation (**Fig. 6 D;** 30.8 ± 30.8%).
304 This difference indicated that other intrinsic or extrinsic factors might exist in mice older
305 than 23 months to promote myeloid-biased hematopoiesis. To investigate this further, we
306 transplanted ten GFP^+ young LT-HSCs into young or 2-year-old recipient mice and
307 examined their PB (**Fig. 7 A**). We limited the observation period to 12 weeks because
308 many aged recipient mice had died prior to that point (**Fig. 7 B**). PB analysis revealed
309 that aged recipient mice receiving young LT-HSCs produced significantly more myeloid
310 cells than young recipient mice (**Fig. 7, C-E**). These results suggested that recipient-
311 dependent extrinsic factors, rather than intrinsic factors of transplanted HSCs, had a
312 greater impact on hematopoietic cell differentiation. Then, we examined BM to determine
313 what extrinsic factors affected differentiation of transplanted HSCs. Percentages of CMP
314 and GMP, downstream components of myeloid differentiation, were stable or
315 significantly lower in aged recipient mice than in young recipient mice, just as they were
316 in non-treated aged mice (**Fig. 7 F; Fig. 1 B**). In addition, the percentage of CLP, a
317 downstream component of lymphoid differentiation, did not differ between young and
318 aged recipients (**Fig. 7 F**). In contrast to previous studies (Pinho et al., 2018; Ergen et al.,
319 2012), these findings suggested that intramedullary age-associated changes may not have
320 a significant impact on LT-HSC differentiation.
321 Thymi and spleens of recipient mice were then examined, as these are the structures of
322 lymphoid maturation and production of lymphoid progenitors following migration from
323 BM and prior to their appearance in PB. Donor cells were not microscopically detectable
324 in the majority of aged recipient mice (**Fig. 7, G and I**), and quantitative analysis using a
325 flow cytometer revealed that the frequency of donor cells in spleens and thymi of aged

326 recipients was significantly lower than in young recipients (**Fig. 7, H and J**). These
327 results indicated that the process of lymphoid lineage differentiation was impaired in the
328 spleens and thymi of aged mice compared to young mice, resulting in enhanced myeloid-
329 biased hematopoiesis in PB due to a decrease in the *de novo* lymphocyte production.
330

331 **Discussion**

332 Age-related, myeloid-biased hematopoiesis has been suggested as a potential reason for
333 the decline in acquired immunity in the elderly (Geiger et al., 2013). This process has
334 been linked to an increase in myeloid-biased HSC clones in the bulk-HSC fraction
335 identified by surface antigens through aging. By isolating LT-HSCs and ST-HSCs,
336 respectively, we discovered that age-related changes in the ratio of ST-HSCs to LT-HSCs
337 in bulk-HSCs is responsible for myeloid-biased hematopoiesis.
338 When aged bulk-HSCs were transplanted into young mice, post-transplant hematopoiesis
339 in recipient mice was significantly biased toward myeloid in PB compared to
340 transplantation of young bulk-HSCs (Beerman et al., 2010; Dykstra et al., 2011; Sudo et
341 al., 2000). Historically, this myeloid-biased hematopoiesis derived from aged bulk-HSCs
342 has been considered as evidence supporting expansion of myeloid-biased HSC clones
343 with aging (Geiger et al., 2013; de Haan and Lazare 2018). Other studies, however,
344 suggest that blockage of lymphoid hematopoiesis in aged mice results in myeloid-skewed
345 hematopoiesis through alternative mechanisms (Montecino-Rodriguez et al., 2019). To
346 clarify the cause for this disparity, we chose to examine the LT-HSC fraction, which
347 persists in the BM for long periods of time and is enriched for aging-related alterations.
348 We discovered that post-transplant hematopoiesis of aged LT-HSCs did not vary from
349 that of young LT-HSCs in terms of differentiation capacity. Expression of myeloid-

350 related genes was not significantly altered when LT-HSCs from young and aged mice
351 were compared. Therefore, we inferred that age-related myeloid-biased hematopoiesis
352 cannot be attributed to an increase in myeloid-biased HSCs, at least among LT-HSCs.
353 Given that bulk-HSCs consist of LT-HSCs and ST-HSCs, and that LT-HSCs exhibit no
354 change in differentiation potential with age, we hypothesized that ST-HSCs may be
355 responsible for the myeloid-skewing phenotype in PB. Transcriptomic analysis revealed
356 no enrichment of myeloid-related genes in the ST-HSC fraction, ruling out the possibility
357 of an increase in myeloid-biased HSCs in the ST-HSC fraction. Alternatively, we
358 observed a proportionate decrease in ST-HSCs in bulk-HSCs accompanying an increase
359 in LT-HSCs. We postulated that this relative decrease in ST-HSC ratio is responsible for
360 myeloid-biased hematopoiesis. When isolated LT-HSCs and ST-HSCs from young mice
361 were reconstituted to replicate an aged BM type in terms of the LT-HSC/ST-HSC ratio,
362 we discovered that PB was strongly skewed towards myeloid cells after transplantation
363 of reconstituted HSCs. In contrast, transplantation of reconstituted HSCs with a young
364 BM type resulted in a significantly lymphoid-skewed PB profile.
365 On the other hand, it has been reported that myeloid-biased HSCs have a more persistent
366 capacity for self-renewal (Muller-Sieburg et al., 2004). In fact, in our prior investigation
367 comparing PB 16 weeks post-transplant, myeloid cell production in PB was greater when
368 LT-HSCs were transplanted, while ST-HSC transplantation resulted in a considerable
369 increase in lymphoid cell production (Chen et al., 2016). It is therefore possible that the
370 LT-HSCs and ST-HSCs we isolated utilizing the Hoxb5 reporter system are myeloid- and
371 lymphoid-biased HSCs, respectively. However, the myeloid-producing capacity of LT-
372 HSCs and ST-HSCs 4 weeks post-transplantation is equivalent (Chen et al., 2016). In
373 contrast, 16 weeks after transplantation, ST-HSC transplant recipients demonstrate

374 negligible myeloid development and a predominance of lymphocytes, unlike LT-HSC
375 transplant recipients (Chen et al., 2016). These characteristics show that early post-
376 transplant ST-HSCs lack the phenotypic of lymphoid-biased HSCs. When ST-HSC-
377 transplanted BM cells are employed as donors for secondary transplantation, no donor-
378 cell-derived hematopoiesis is detected in recipients (Chen et al., 2016). In addition, HSCs
379 are not observed in the BM following transplantation of ST-HSCs (**Fig. 5**). These results
380 indicate that ST-HSCs lose their capacity for self-renewal earlier after transplantation
381 than LT-HSCs. In addition, phenotypic examination of lymphocytes in PB after ST-HSC
382 transplantation revealed that nearly all of them were memory cells, and that there was no
383 *de novo* supply of T cells. In other words, ST-HSCs may have been erroneously classified
384 as lymphoid-biased HSCs due to the preservation of memory lymphocytes with a long
385 half-life in the peripheral circulation, despite the absence of *de novo* hematopoiesis
386 following transplantation of ST-HSCs. These findings suggest that the bias toward
387 myeloid and lymphoid lineages in post-transplant PB is not regulated by heterogeneity of
388 multipotency, but by heterogeneity of self-renewal capacity.
389 Multiple extrinsic factors have been implicated as HSC-independent causes of myeloid-
390 biased hematopoiesis associated with aging. Some findings suggest that cell interaction
391 with niche cells in BM is altered (Pinho et al., 2018), whereas others claim that chronic
392 inflammation in aged mice lowers production of lymphoid progenitors and induces
393 myeloid-biased hematopoiesis (Montecino-Rodriguez et al., 2019; Ergen et al., 2012). To
394 identify HSC-independent causes of myeloid-biased hematopoiesis specifically, we
395 transplanted young LT-HSCs into young or aged mice. Cellular differentiation observed
396 in BM revealed that proportions of GMP, MEP, and CLP are unchanged between young
397 and aged recipients. In contrast, an examination of spleens and thymi, the sites of

398 lymphocyte maturation, revealed the absence of donor cells in aged recipients. These
399 findings suggest that myeloid cells increase in aging mice due to a relative decrease in
400 the ratio of mature lymphocytes in PB, resulting from inhibition of lymphocyte
401 maturation outside the BM, such as in the thymus and spleen, rather than a significant
402 change in cell differentiation caused by the intramedullary environment. Attempts have
403 been made in the past to restore thymus function in aged mice by administering
404 keratinocyte growth factor (KGF) (S. W. Rossi et al., 2007). Indeed, in aged mice,
405 lymphocyte hematopoiesis recovers, which is consistent with our results that the
406 extramedullary environment influences the myeloid-bias phenotype in PB (S. W. Rossi
407 et al., 2007).
408 It has been clinically documented that recovery of the lymphocyte fraction in PB is
409 delayed in elderly donors, compared to young donors (González-Vicent et al., 2017;
410 Baron et al., 2006). Although it is undeniable that this phenomenon may be due to
411 decreased HSC hematopoietic potential, it may also be due to a change in the ratio of LT-
412 HSC/ST-HSCs in bulk-HSCs, as described in our report, which may give the appearance
413 of a myeloid bias in PB after transplantation. It has also been noted that lymphocyte
414 recovery is delayed in elderly patients compared to younger patients (Berger et al., 2008;
415 van der Maas et al., 2021). Age-related loss in thymus and spleen functions has been
416 recorded in humans, implying that the same mechanism is acting as in our mouse
417 observations. If it is possible to assess and regulate the LT-HSC/ST-HSC ratio in donors
418 and thymus/spleen function in recipients in the future, it will help to develop accurate
419 models for predicting lymphocyte recovery after transplantation as well as new
420 transplantation strategies.

421 In summary, we have demonstrated for the first time that the ratio of LT-HSC/ST-HSC
422 is important in age-related myeloid skewed hematopoiesis as an HSC-dependent factor
423 and that aging-related thymus and spleen dysfunction also contributes significantly as an
424 HSC-independent factor. Furthermore, here we propose a "self-renewal heterogeneity
425 model" as a new mechanism for hematopoietic heterogeneity, including myeloid-biased
426 hematopoiesis in aged mice (**Fig. 8**). In addition to this report, we have also shown that
427 cellular differentiation in the PB after transplantation can vary by changing
428 transplantation conditions, ultimately altering self-renewal ability (Sakamaki et al., 2021;
429 Nishi et al., 2022). This highlights the significance of deciphering molecular processes
430 that regulate the heterogeneity of HSC self-renewal capacity, which will help to provide
431 a better understanding of the hematopoietic system and the hematopoietic hierarchy in
432 the future.
433
434 **Methods**
435 **Mice**
436 Mice with an *Hoxb5*-tri-mCherry (C57BL/6J background), derived from our previous
437 work (Chen et al., 2016), were harvested for donor cells for transplantation, PB, and BM
438 analysis. CAG-EGFP mice (C57BL/6J background) were bred with *Hoxb5*-tri-mCherry
439 for transplantation experiments. 8-14-week-old C57BL/6-Ly5.1 mice (purchased from
440 Sankyo Labo Service) were used as recipients for transplantation assays. For aged
441 recipients, 2-year-old CD45.2 C57BL/6J mice were purchased from CLEA Japan.
442 Supporting BM cells were collected from 8-12-week-old C57BL/6-Ly5.1 × C57BL/6J
443 (F_1 mice $CD45.1^+/CD45.2^+$). All mice were housed in specific pathogen-free (SPF)
444 conditions and were carefully observed by staff members. Mice were bred according to

445 RIKEN or Kyoto University. All animal protocols were approved by the RIKEN Center
446 for Biosystems Dynamics Research and Kyoto University.
447
448 **Flow cytometry, cell sorting, and bone marrow analyses**
449 Flow cytometry and cell sorting were performed on a FACS Aria II cell sorter (BD
450 Biosciences) and analyzed using FlowJo™ software (BD Biosciences). Bone marrow
451 (BM) cells were collected from bilateral tibias, femurs, humeri, and pelvises in Ca^{2+}- and
452 Mg^{2+}-free PBS supplemented with 2% heat-inactivated bovine serum (Gibco) and 2 mM
453 EDTA (Thermo Fisher Scientific). Cells were passed through 100-µm, and 40-µm
454 strainers (Corning) before analysis and sorting. Prior to staining, samples were blocked
455 with 50 ug/mL rat IgG (Sigma-Aldrich) for 15 min. To enrich HSCs and progenitor
456 populations for sorting and bone marrow analyses, cells were stained with APC-
457 eFluor780-conjugated anti-c-Kit (clone: 2B8) and fractionated using anti-APC magnetic
458 beads and LS columns (both Miltenyi Biotec). c-Kit^{+} cells were then stained with
459 combinations of antibodies as described in Supplemental Table 1. All staining was
460 incubated at 4°C for 30 min, except for CD34 staining, which was incubated for 90 min.
461 Samples were washed twice after staining. Prior to flow cytometry or cell sorting, samples
462 were stained with SYTOX Red Dead Cell Stain (Life Technologies) or 7-
463 aminoactinomycin D (BioLegend). Cells were double sorted for purity.
464
465 **Transplantation and peripheral blood analyses**
466 12-24 hours prior to transplantation, C57BL/6-Ly5.1 mice, or aged C57BL/6J recipient
467 mice were lethally irradiated with single doses of 8.7 Gy or 9.1Gy. For transplantation
468 assays, donor cells were first combined with 2×10^5 whole bone marrow supporting cells

469 (C57BL/6-Ly5.1 × C57BL/6J F_1 mice $CD45.1^+/CD45.2^+$) in 200 μL of PBS with 2%
470 FBS, and then injected into the retro-orbital venous plexus. For evaluation of post-
471 transplant kinetics, PB was collected and analyzed. At each time point, 50 μL of blood
472 were collected from the tail vein and re-suspended in Ca^{2+}- and Mg^{2+}-free PBS
473 supplemented with 2 mM EDTA. Red blood cells were lysed twice on ice for 3 min with
474 BD Pharm Lyse Buffer (BD Pharmingen). Identification of leukocyte subsets was
475 performed by staining with antibodies. Antibody information was described in
476 Supplemental Table 1. For evaluation of lineage output, the frequency of each lineage
477 (NK cell, B cell, T cell, neutrophil, and monocyte) was determined in the whole fraction.
478 The analysis of donor lineage output was restricted to donor cells showing ≥ 0.1% donor
479 chimerism at the last PB analysis to allow reliable detection. The percentage of donor
480 chimerism in PB was defined as the percentage of $CD45.1^-CD45.2^+$ cells among total
481 $CD45.1^-CD45.2^+$ and $CD45.1^+CD45.2^+$ cells. PB data represents mice which survived
482 until the last PB analysis.
483
484 **Thymus and Spleen analysis**
485 Thymi and spleens were harvested and disrupted into a single cell suspension. Cells were
486 passed through 100-μm, and 40-μm strainers (Corning). Isolated thymocytes and
487 splenocytes were incubated on ice for 30 min with appropriately diluted antibodies in
488 staining buffer. Identification of B cells in spleens and T cells in thymi was performed
489 by staining with antibodies described in Supplemental Table 1. Prior to flow cytometry
490 or cell sorting, samples were stained with SYTOX Red Dead Cell Stain (Life
491 Technologies).
492

493 **Tissue imaging**

494 Freshly dissected spleens and thymi were fixed in 4% PFA (Nacalai tesque) in PBS for
495 24 h at 4°C. After PFA washout with PBS, tissues were cryoprotected with 30% sucrose
496 in PBS for 24 h at 4°C, embedded in Tissue-Tek O.C.T. compound (Sakura Finetek), and
497 snap-frozen in liquid nitrogen. Serial 10-μm longitudinal cryostat sections were obtained
498 using CryoStar NX50 (Thermo Fisher Scientific). Cell nuclei were counterstained with
499 4',6-diamidino-2-phenylindole (DAPI, 1 μg/mL, Roche). To reduce autofluorescence,
500 tissue sections were treated with Vector TrueVIEW autofluorescence quenching kit
501 (Vector Laboratories). Images were obtained from Leica TCS SP8 (Leica).

502

503 **RNA sequencing**

504 Total RNA was isolated with Trizol (Thermo Fisher Scientific) and cleaned up using
505 RNeasy MinElute columns (QIAGEN). cDNA libraries were prepared from bulk-HSCs,
506 ST-HSCs and LT-HSCs using a KAPA RNA HyperPrep kit with RiboErase (HMR)
507 (Kapa Biosystems) and sequenced using a Hiseq 1500 (Illumina) to obtain 2 × 127 base-
508 pair (bp) paired-end reads. Three replicates were sequenced for each population. Raw
509 transcriptome sequence data were mapped to the genome (mm10) using HISAT2 (ver
510 2.1.0) (Kim et al., 2015). Alignments were then passed to StringTie (ver 1.3.4d), which
511 was used to assemble and quantify transcripts in each sample (Pertea et al., 2016). EdgeR
512 (ver 3.22.5) was then used to compare all transcripts across conditions and to produce
513 tables and plots of differentially expressed genes and transcripts (Robinson et al., 2009).
514 Normalization with the TMM method was performed with the edgeR package in
515 Bioconductor (https://bioconductor.org/). Genes (12,808 genes) were selected for
516 hierarchical clustering based on the mean of TMM normalized read counts across all

517 samples' cells (mean ≥ 1). Then, clustering was performed by using the hclust function
518 for R (distance = Spearman's correlation'; method = 'ward.D2'). We depicted Venn
519 diagrams and performed GSEA analyses in Figures 4D-G and S4C-D using previously
520 published gene sets after excluding genes that could not be annotated by our
521 transcriptome dataset. GSEA was performed using GSEA software
522 (http://www.broadinstitute.org/gsea) with default settings (Subramanian et al., 2005).
523

524 **Quantification and statistical analyses**

525 Statistical analyses were performed using ggplot2 in R (version 4.1.2) or Microsoft Excel.
526 Sample size for each experiment and replicate numbers of experiments are included in
527 figure legends. Statistical significance was determined using Welch's t test. P values <
528 0.05 were considered significant.
529

530 **Data and materials availability**

531 Sequencing data has been deposited in the Gene Expression Omnibus under accession
532 code GSE226803. Correspondence and requests for materials should be addressed to
533 M.M. (miya75@med.kobe-u.ac.jp).
534

535 **Acknowledgements**

536 We gratefully acknowledge Hiroshi Kiyonari for animal care and providing recipient
537 mice at RIKEN BDR. Shigehiro Kuraku, Mitsutaka Kadota, and Chiharu Tanegashima
538 provided technical support for RNA sequencing and analysis at RIKEN BDR. Momo
539 Fujii performed imaging experiments at RIKEN BDR. Hitomi Oga, Kayoko Nagasaka,
540 and Masaki Miyahashi provided laboratory management at Kobe University. The authors

gratefully acknowledge ongoing support for this work: Masanori Miyanishi was supported by the Japan Society for the Promotion of Science (JSPS) KAKENHI Grant Number JP17K07407 and JP20H03268, The Mochida Memorial Foundation for Medical and Pharmaceutical Research, The Life Science Foundation of Japan, The Takeda Science Foundation, The Astellas Foundation for Research on Metabolic Disorders, AMED-PRIME, AMED under Grant Number JP18gm6110020. Taro Sakamaki was supported by the JSPS Core-to-Core Program, JSPS KAKENHI Grant Numbers JP21K20669, JP22K16334, RIKEN Junior Research Associate Program. Katsuyuki Nishi was supported by JSPS Grant Numbers KAKENHI JP18J13408 and 23K15326.

Authorship Contributions

K.N. conceived, performed, analyzed the experiments. T.S. and K.S. performed transplantation experiments. M.M. conceived, performed, analyzed, and oversaw the experiments. K.N. and M.M. wrote the manuscript. T.S., A.N., K.S.K., K.S., M.A., N.Y., and A.T. provided comments on the manuscript.

Disclosure of Conflicts of Interest

The authors declare no conflicts of interest in relation to the present study.

References

Baron, Frédéric, Barry Storer, Michael B. Maris, Jan Storek, Fanny Piette, Monja Metcalf, Kristen White, et al. 2006. "Unrelated Donor Status and High Donor Age Independently Affect Immunologic Recovery after Nonmyeloablative Conditioning." *Biology of Blood and Marrow Transplantation* 12 (11): 1176–87. https://doi.org/10.1016/j.bbmt.2006.07.004.

Beerman, Isabel, Deepta Bhattacharya, Sasan Zandi, Mikael Sigvardsson, Irving L. Weissman, David Brydere, and Derrick J. Rossia. 2010. "Functionally Distinct Hematopoietic Stem Cells Modulate Hematopoietic Lineage Potential during

Aging by a Mechanism of Clonal Expansion." *Proceedings of the National Academy of Sciences of the United States of America* 107 (12): 5465–70. https://doi.org/10.1073/pnas.1000834107.

Berger, Massimo, O. Figari, B. Bruno, A. Raiola, A. Dominietto, M. Fiorone, M. Podesta, et al. 2008. "Lymphocyte Subsets Recovery Following Allogeneic Bone Marrow Transplantation (BMT): CD4+ Cell Count and Transplant-Related Mortality." *Bone Marrow Transplantation* 41 (1): 55–62. https://doi.org/10.1038/sj.bmt.1705870.

Busch, Katrin, Kay Klapproth, Melania Barile, Michael Flossdorf, Tim Holland-Letz, Susan M. Schlenner, Michael Reth, Thomas Höfer, and Hans Reimer Rodewald. 2015. "Fundamental Properties of Unperturbed Haematopoiesis from Stem Cells in Vivo." *Nature* 518 (7540): 542–46. https://doi.org/10.1038/nature14242.

Challen, Grant A., Nathan C. Boles, Stuart M. Chambers, and Margaret A. Goodell. 2010. "Distinct Hematopoietic Stem Cell Subtypes Are Differentially Regulated by TGF-B1." *Cell Stem Cell* 6 (3): 265–78. https://doi.org/10.1016/j.stem.2010.02.002.

Chambers, Stuart M., Nathan C. Boles, Kuan Yin K. Lin, Megan P. Tierney, Teresa V. Bowman, Steven B. Bradfute, Alice J. Chen, et al. 2007. "Hematopoietic Fingerprints: An Expression Database of Stem Cells and Their Progeny." *Cell Stem Cell* 1 (5): 578–91. https://doi.org/10.1016/j.stem.2007.10.003.

Chen, James Y., Masanori Miyanishi, Sean K. Wang, Satoshi Yamazaki, Rahul Sinha, Kevin S. Kao, Jun Seita, Debashis Sahoo, Hiromitsu Nakauchi, and Irving L. Weissman. 2016. "Hoxb5 Marks Long-Term Haematopoietic Stem Cells and Reveals a Homogenous Perivascular Niche." *Nature* 530 (7589): 223–27. https://doi.org/10.1038/nature16943.

Cho, Rebecca H., Hans B. Sieburg, and Christa E. Muller-Sieburg. 2008. "A New Mechanism for the Aging of Hematopoietic Stem Cells: Aging Changes the Clonal Composition of the Stem Cell Compartment but Not Individual Stem Cells." *Blood* 111 (12): 5553–61. https://doi.org/10.1182/blood-2007-11-123547.

Crooke, Stephen N., Inna G. Ovsyannikova, Gregory A. Poland, and Richard B. Kennedy. 2019. "Immunosenescence and Human Vaccine Immune Responses." *Immunity & Ageing* 16 (1): 1–16. https://doi.org/10.1186/s12979-019-0164-9.

Dorshkind, Kenneth, Thomas Höfer, Encarnacion Montecino-Rodriguez, Peter D. Pioli, and Hans Reimer Rodewald. 2020. "Do Haematopoietic Stem Cells Age?" *Nature Reviews Immunology* 20 (3): 196–202. https://doi.org/10.1038/s41577-019-0236-2.

Dykstra, Brad, Sandra Olthof, Jaring Schreuder, Martha Ritsema, and Gerald de Haan. 2011. "Clonal Analysis Reveals Multiple Functional Defects of Aged Murine Hematopoietic Stem Cells." *The Journal of Experimental Medicine* 208 (13): 2691–2703. https://doi.org/10.1084/jem.20111490.

Dykstra, Brad, Sandra Olthof, Jaring Schreuder, Martha Ritsema, and Gerald De Haan. 2011. "Clonal Analysis Reveals Multiple Functional Defects of Aged Murine Hematopoietic Stem Cells." *Journal of Experimental Medicine* 208 (13): 2691–2703. https://doi.org/10.1084/jem.20111490.

Ergen, Aysegul V., Nathan C. Boles, and Margaret A. Goodell. 2012. "Rantes/Ccl5 Influences Hematopoietic Stem Cell Subtypes and Causes Myeloid Skewing." *Blood* 119 (11): 2500–2509. https://doi.org/10.1182/blood-2011-11-391730.

Flohr Svendsen, Arthur, Daozheng Yang, Kyung Mok Kim, Seka Lazare, Natalia Skinder, Erik Zwart, Anna Mura-Meszaros, et al. 2021. "A Comprehensive Transcriptome Signature of Murine Hematopoietic Stem Cell Aging." *Blood* 138 (6): 439–51. https://doi.org/10.1182/blood.2020009729.

Geiger, Hartmut, Gerald De Haan, and M. Carolina Florian. 2013. "The Ageing Haematopoietic Stem Cell Compartment." *Nature Reviews Immunology* 13 (5): 376–89. https://doi.org/10.1038/nri3433.

González-Vicent, Marta, Blanca Molina, Natalia Deltoro, Julián Sevilla, José Luis Vicario, Ana Castillo, Manuel Ramirez, and Miguel Ángel Díaz. 2017. "Donor Age Matters in T-Cell Depleted Haploidentical Hematopoietic Stem Cell Transplantation in Pediatric Patients: Faster Immune Reconstitution Using Younger Donors." *Leukemia Research* 57: 60–64. https://doi.org/10.1016/j.leukres.2017.03.001.

Grover, Amit, Alejandra Sanjuan-Pla, Supat Thongjuea, Joana Carrelha, Alice Giustacchini, Adriana Gambardella, Iain Macaulay, et al. 2016. "Single-Cell RNA Sequencing Reveals Molecular and Functional Platelet Bias of Aged Haematopoietic Stem Cells." *Nature Communications* 7. https://doi.org/10.1038/ncomms11075.

Haan, Gerald de, and Seka Simone Lazare. 2018. "Aging of Hematopoietic Stem Cells." *Blood* 131 (5): 479–87. https://doi.org/10.1182/blood-2017-06-746412.

Haan, Gerald De, and Seka Simone Lazare. 2018. "Aging of Hematopoietic Stem Cells." www.bloodjournal.org.

Jones, D. Leanne, and Thomas A. Rando. 2011. "Emerging Models and Paradigms for Stem Cell Ageing." *Nature Cell Biology* 13 (5): 506–12. https://doi.org/10.1038/ncb0511-506.

Kim, Daehwan, Ben Langmead, and Steven L. Salzberg. 2015. "HISAT: A Fast Spliced Aligner with Low Memory Requirements." *Nature Methods* 12 (4): 357–60. https://doi.org/10.1038/nmeth.3317.

Kowalczyk, Monika S., Itay Tirosh, Dirk Heckl, Tata Nageswara Rao, Atray Dixit, Brian J. Haas, Rebekka K. Schneider, Amy J. Wagers, Benjamin L. Ebert, and Aviv Regev. 2015. "Single-Cell RNA-Seq Reveals Changes in Cell Cycle and Differentiation Programs upon Aging of Hematopoietic Stem Cells." *Genome Research* 25 (12): 1860–72. https://doi.org/10.1101/gr.192237.115.

Liberzon, Arthur, Chet Birger, Helga Thorvaldsdóttir, Mahmoud Ghandi, Jill P. Mesirov, and Pablo Tamayo. 2015. "The Molecular Signatures Database Hallmark Gene Set Collection." *Cell Systems* 1 (6): 417–25. https://doi.org/10.1016/j.cels.2015.12.004.

Maas, Nicolaas G. van der, Erik G.J. von Asmuth, Dagmar Berghuis, Pauline A. van Schouwenburg, Hein Putter, Mirjam van der Burg, and Arjan C. Lankester. 2021. "Modeling Influencing Factors in B-Cell Reconstitution After Hematopoietic Stem Cell Transplantation in Children." *Frontiers in Immunology* 12 (May): 1–8. https://doi.org/10.3389/fimmu.2021.684147.

Majeti, Ravindra, Christopher Y. Park, and Irving L. Weissman. 2007. "Identification of a Hierarchy of Multipotent Hematopoietic Progenitors in Human Cord Blood." *Cell Stem Cell* 1 (6): 635–45. https://doi.org/10.1016/j.stem.2007.10.001.

Mann, Mati, Arnav Mehta, Carl G de Boer, Monika S Kowalczyk, Kevin Lee, Pearce Haldeman, Noga Rogel, et al. 2018. "Heterogeneous Responses of Hematopoietic

Stem Cells to Inflammatory Stimuli Are Altered with Age." *Cell Reports* 25 (11): 2992–3005. https://doi.org/10.1016/j.celrep.2018.11.056.

Mejia-Ramirez, Eva, and Maria Carolina Florian. 2020. "Understanding Intrinsic Hematopoietic Stem Cell Aging." *Haematologica* 105 (1): 22–37. https://doi.org/10.3324/haematol.2018.211342.

Min, Hyeyoung, Encarnacion Montecino-Rodriguez, and Kenneth Dorshkind. 2006. "Effects of Aging on the Common Lymphoid Progenitor to Pro-B Cell Transition." *The Journal of Immunology* 176 (2): 1007–12. https://doi.org/10.4049/jimmunol.176.2.1007.

Montecino-Rodriguez, Encarnacion, Ying Kong, David Casero, Adrien Rouault, Kenneth Dorshkind, and Peter D. Pioli. 2019. "Lymphoid-Biased Hematopoietic Stem Cells Are Maintained with Age and Efficiently Generate Lymphoid Progeny." *Stem Cell Reports* 12 (3): 584–96. https://doi.org/10.1016/j.stemcr.2019.01.016.

Morrison, Sean J., and Irving L. Weissman. 1994. "The Long-Term Repopulating Subset of Hematopoietic Stem Cells Is Deterministic and Isolatable by Phenotype." *Immunity* 1 (8): 661–73. https://doi.org/10.1016/1074-7613(94)90037-X.

Morrison, Sean J, A M Wandycz, K Akashi, A Globerson, and Irving L Weissman. 1996. "The Aging of Hematopoietic Stem Cells." *Nature Medicine* 2 (9): 1011–16. https://doi.org/10.1038/nm0996-1011.

Muller-Sieburg, Christa E., Rebecca H. Cho, Lars Karlsson, Jing F. Huang, and Hans B. Sieburg. 2004. "Myeloid-Biased Hematopoietic Stem Cells Have Extensive Self-Renewal Capacity but Generate Diminished Lymphoid Progeny with Impaired IL-7 Responsiveness." *Blood* 103 (11): 4111–18. https://doi.org/10.1182/blood-2003-10-3448.

Nilsson, Alexandra Rundberg, Shamit Soneji, Sofia Adolfsson, David Bryder, and Cornelis Jan Pronk. 2016. "Human and Murine Hematopoietic Stem Cell Aging Is Associated with Functional Impairments and Intrinsic Megakaryocytic/Erythroid Bias." *PLoS ONE* 11 (7): 1–20. https://doi.org/10.1371/journal.pone.0158369.

Nishi, Katsuyuki, Taro Sakamaki, Kay Sadaoka, Momo Fujii, Akifumi Takaori-Kondo, James Y. Chen, and Masanori Miyanishi. 2022. "Identification of the Minimum Requirements for Successful Haematopoietic Stem Cell Transplantation." *British Journal of Haematology* 196 (3): 711–23. https://doi.org/10.1111/bjh.17867.

Pang, Wendy W., Elizabeth A. Price, Debashis Sahoo, Isabel Beerman, William J. Maloney, Derrick J. Rossi, Stanley L. Schrier, and Irving L. Weissman. 2011. "Human Bone Marrow Hematopoietic Stem Cells Are Increased in Frequency and Myeloid-Biased with Age." *Proceedings of the National Academy of Sciences of the United States of America* 108 (50): 20012–17. https://doi.org/10.1073/pnas.1116110108.

Pertea, Mihaela, Daehwan Kim, Geo M. Pertea, Jeffrey T. Leek, and Steven L. Salzberg. 2016. "Transcript-Level Expression Analysis of RNA-Seq Experiments with HISAT, StringTie and Ballgown." *Nature Protocols* 11 (9): 1650–67. https://doi.org/10.1038/nprot.2016.095.

Pietras, Eric M. 2017. "Inflammation: A Key Regulator of Hematopoietic Stem Cell Fate in Health and Disease." *Blood* 130 (15): 1693–98. https://doi.org/10.1182/blood-2017-06-780882.

Pinho, Sandra, Tony Marchand, Eva Yang, Qiaozhi Wei, Claus Nerlov, and Paul S. Frenette. 2018. "Lineage-Biased Hematopoietic Stem Cells Are Regulated by Distinct Niches." *Developmental Cell* 44 (5): 634-641.e4. https://doi.org/10.1016/j.devcel.2018.01.016.

Pronk, Cornelis J.H., Derrick J. Rossi, Robert Månsson, Joanne L. Attema, Gudmundur Logi Norddahl, Charles Kwok Fai Chan, Mikael Sigvardsson, Irving L. Weissman, and David Bryder. 2007. "Elucidation of the Phenotypic, Functional, and Molecular Topography of a Myeloerythroid Progenitor Cell Hierarchy." *Cell Stem Cell* 1 (4): 428–42. https://doi.org/10.1016/j.stem.2007.07.005.

Robinson, Mark D., Davis J. McCarthy, and Gordon K. Smyth. 2009. "EdgeR: A Bioconductor Package for Differential Expression Analysis of Digital Gene Expression Data." *Bioinformatics* 26 (1): 139–40. https://doi.org/10.1093/bioinformatics/btp616.

Rossi, Derrick J., David Bryder, Jun Seita, Andre Nussenzweig, Jan Hoeijmakers, and Irving L. Weissman. 2007. "Deficiencies in DNA Damage Repair Limit the Function of Haematopoietic Stem Cells with Age." *Nature* 447 (7145): 725–29. https://doi.org/10.1038/nature05862.

Rossi, Derrick J., Catriona H.M. Jamieson, and Irving L. Weissman. 2008. "Stems Cells and the Pathways to Aging and Cancer." *Cell* 132 (4): 681–96. https://doi.org/10.1016/j.cell.2008.01.036.

Rossi, Derrick J, David Bryder, Jacob M Zahn, Henrik Ahlenius, Rebecca Sonu, Amy J Wagers, and Irving L Weissman. 2005. "Cell Intrinsic Alterations Underlie Hematopoietic Stem Cell Aging." *Proceedings of the National Academy of Sciences of the United States of America* 102 (26): 9194–99. https://doi.org/10.1073/pnas.0503280102.

Rossi, Simona W., Lukas T. Jeker, Tomoo Ueno, Sachiyo Kuse, Marcel P. Keller, Saulius Zuklys, Andrei V. Gudkov, et al. 2007. "Keratinocyte Growth Factor (KGF) Enhances Postnatal T-Cell Development via Enhancements in Proliferation and Function of Thymic Epithelial Cells." *Blood* 109 (9): 3803–11. https://doi.org/10.1182/blood-2006-10-049767.

Sakamaki, Taro, Kevin S. Kao, Katsuyuki Nishi, James Y. Chen, Kay Sadaoka, Momo Fujii, Akifumi Takaori-Kondo, Irving L. Weissman, and Masanori Miyanishi. 2021. "Hoxb5 Defines the Heterogeneity of Self-Renewal Capacity in the Hematopoietic Stem Cell Compartment." *Biochemical and Biophysical Research Communications* 539 (February): 34–41. https://doi.org/10.1016/j.bbrc.2020.12.077.

Sanjuan-Pla, Alejandra, Iain C. Macaulay, Christina T. Jensen, Petter S. Woll, Tiago C. Luis, Adam Mead, Susan Moore, et al. 2013. "Platelet-Biased Stem Cells Reside at the Apex of the Haematopoietic Stem-Cell Hierarchy." *Nature* 502 (7470): 232–36. https://doi.org/10.1038/nature12495.

SanMiguel, Jennifer M., Kira Young, and Jennifer J. Trowbridge. 2020. "Hand in Hand: Intrinsic and Extrinsic Drivers of Aging and Clonal Hematopoiesis." *Experimental Hematology* 91: 1–9. https://doi.org/10.1016/j.exphem.2020.09.197.

Schultz, Michael B., and David A. Sinclair. 2016. "When Stem Cells Grow Old: Phenotypes and Mechanisms of Stem Cell Aging." *Development (Cambridge)* 143 (1): 3–14. https://doi.org/10.1242/dev.130633.

Spangrude, Gerald J., Diane M. Brooks, and Daniel B. Tumas. 1995. "Long-Term Repopulation of Irradiated Mice with Limiting Numbers of Purified Hematopoietic Stem Cells: In Vivo Expansion of Stem Cell Phenotype but Not Function." *Blood* 85 (4): 1006–16. https://doi.org/10.1182/blood.v85.4.1006.bloodjournal8541006.

Spangrude, Gerald J, Shelly Heimfeld, and Irving L Weissman. 1988. "Purification and Characterization of Mouse Hematopoietic Stem Cells." *Science (New York, N.Y.)* 241 (4861): 58–62. https://doi.org/10.1126/science.2898810.

Subramanian, Aravind, Pablo Tamayo, Vamsi K. Mootha, Sayan Mukherjee, Benjamin L. Ebert, Michael A. Gillette, Amanda Paulovich, et al. 2005. "Gene Set Enrichment Analysis: A Knowledge-Based Approach for Interpreting Genome-Wide Expression Profiles." *Proceedings of the National Academy of Sciences of the United States of America* 102 (43): 15545–50. https://doi.org/10.1073/pnas.0506580102.

Sudo, K, H Ema, Y Morita, and H Nakauchi. 2000. "Age-Associated Characteristics of Murine Hematopoietic Stem Cells [In Process Citation]." *J Exp Med* 192 (9): 1273–80.

Webster, Robert G. 2000. "Immunity to Influenza in the Elderly." *Vaccine* 18 (16): 1686–89. https://doi.org/10.1016/S0264-410X(99)00507-1.

Weissman, Irving L., and Judith A. Shizuru. 2008. "The Origins of the Identification and Isolation of Hematopoietic Stem Cells, and Their Capability to Induce Donor-Specific Transplantation Tolerance and Treat Autoimmune Diseases." *Blood* 112 (9): 3543–53. https://doi.org/10.1182/blood-2008-08-078220.

Figure 1.

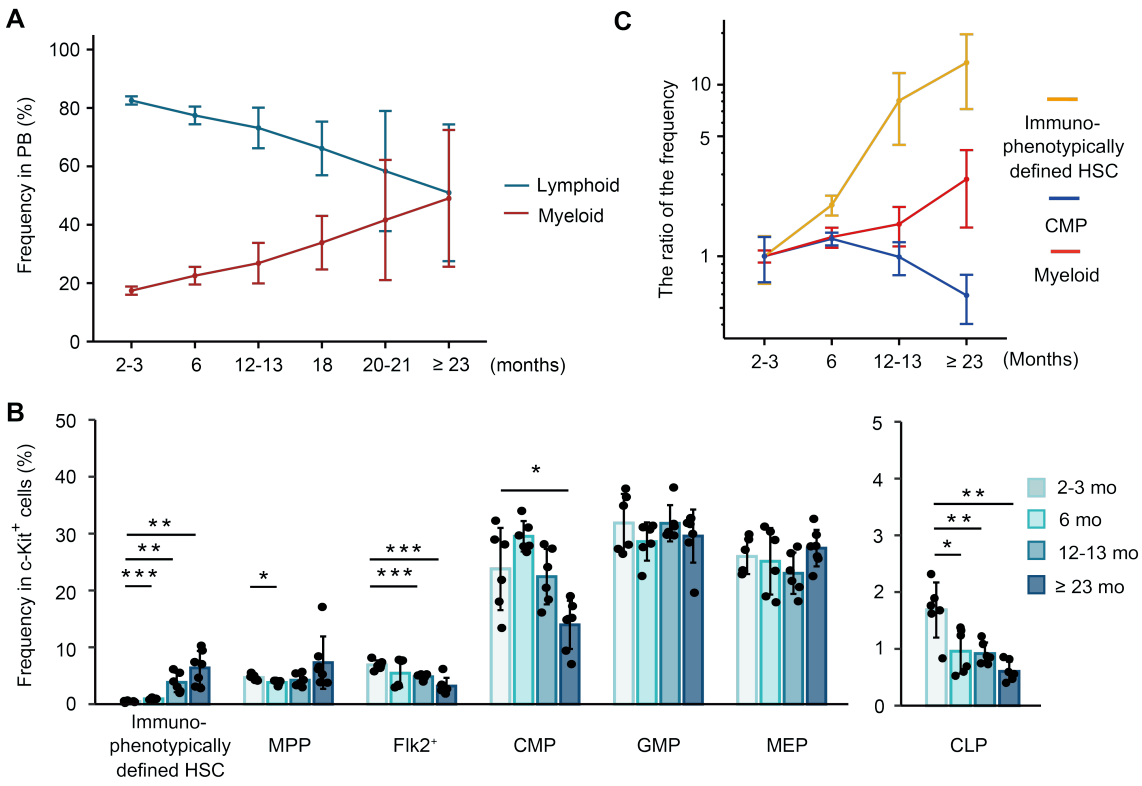

Figure 1. Comprehensive analysis of hematopoietic alternations with age shows a discrepancy of age-associated changes between peripheral blood and bone marrow

(A) Average frequency of myeloid cells (neutrophils, monocytes) and lymphoid cells (B cells, T cells, and NK cells) in PB at the age of 2-3 months (n = 6), 6 months (n = 6), 12-13 months (n = 6), 18 months (n = 6), 20-21 months (n = 5), ≥ 23 months (n = 16). Abbreviation: PB = Peripheral blood.

(B) Average frequency of immunophenotypically defined HSC and progenitor cells in BM of 2-3-month mice (n = 6), 6-month mice (n = 6), 12-13-month mice (n = 6), ≥ 23-month mice (n = 7).

(C) Age-associated changes of immunophenotypically defined HSC and myeloid differentiation components (CMP and myeloid cells in the PB). The ratio of aged to young

frequency was calculated as (the fraction frequency at each aged mice (%)) / (the average fraction frequency at 2-3-month mice (%)). *$P < 0.05$. **$P < 0.01$. ***$P < 0.001$. Data and error bars represent means ± standard deviation.

Figure 2.

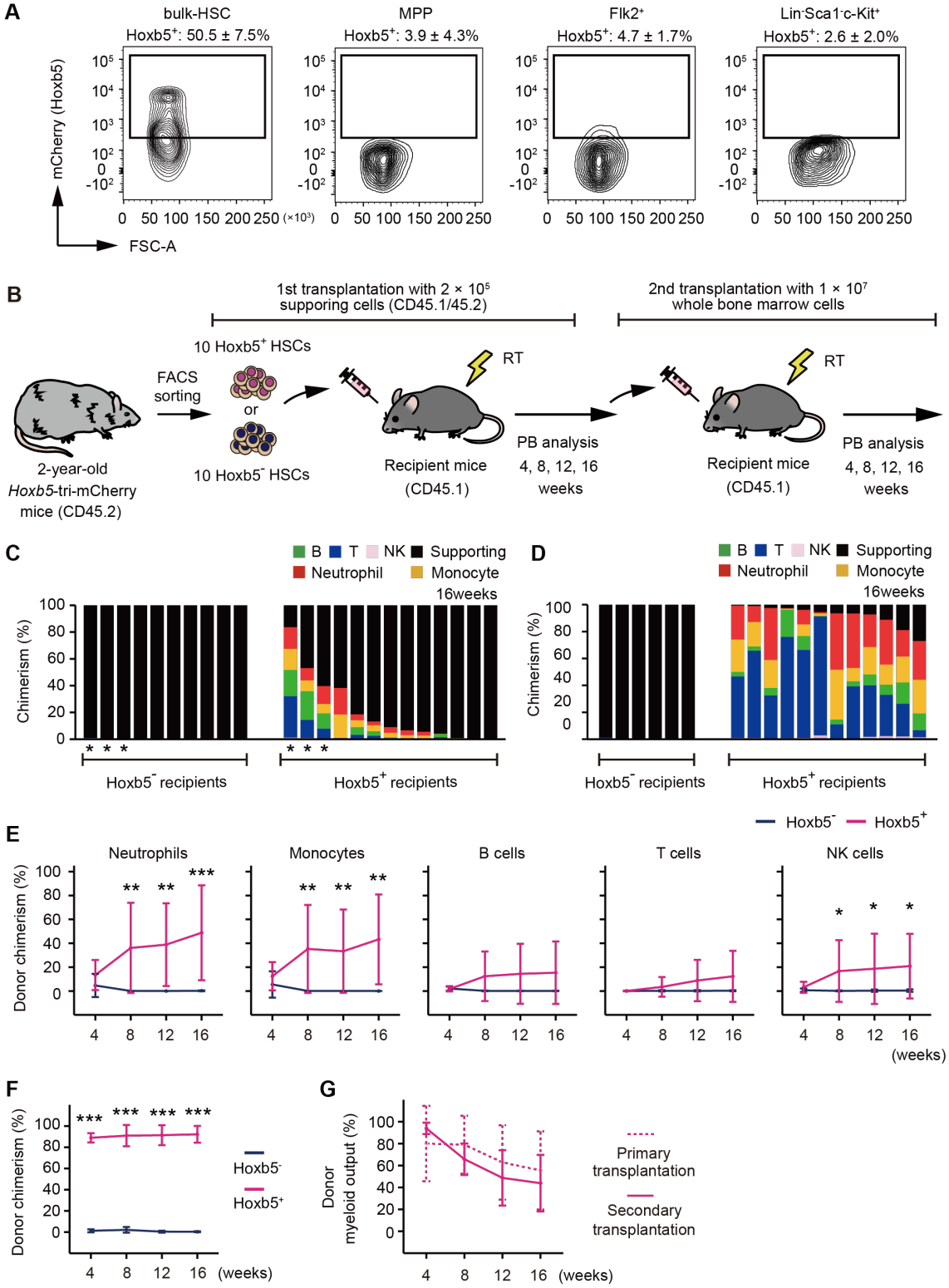
A
bulk-HSC
Hoxb5+: 50.5 ± 7.5%
MPP
Hoxb5+: 3.9 ± 4.3%
Flk2+
Hoxb5+: 4.7 ± 1.7%
Lin-Sca1-c-Kit+
Hoxb5+: 2.6 ± 2.0%
mCherry (Hoxb5)
FSC-A
B
1st transplantation with 2 × 10^5 supporing cells (CD45.1/45.2)
2nd transplantation with 1 × 10^7 whole bone marrow cells
10 Hoxb5+ HSCs
FACS sorting
or
10 Hoxb5- HSCs
2-year-old Hoxb5-tri-mCherry mice (CD45.2)
RT
Recipient mice (CD45.1)
PB analysis 4, 8, 12, 16 weeks
C
D
B T NK Supporting
Neutrophil Monocyte
16weeks
Chimerism (%)
Hoxb5- recipients
Hoxb5+ recipients
E
Hoxb5- Hoxb5+
Neutrophils
Monocytes
B cells
T cells
NK cells
Donor chimerism (%)
(weeks)
F
Donor chimerism (%)
Hoxb5-
Hoxb5+
(weeks)
G
Donor myeloid output (%)
Primary transplantation
Secondary transplantation
(weeks)

861 **Figure 2. The expansion of myeloid-biased clones was not observed in 2-year-old**
862 **LT-HSCs after their transplantation.**
863 (A) Hoxb5 reporter expression in bulk-HSC, MPP, Flk2$^+$, and Lin$^-$Sca1$^-$c-Kit$^+$
864 populations in the 2-year-old *Hoxb5*-tri-mCherry mice. Values indicate the percentage of
865 mCherry$^+$ cells ± standard deviation in each fraction (n = 3).
866 (B) Experimental design to assess the long-term reconstitution ability of Hoxb5$^+$ HSCs or
867 Hoxb5$^-$ HSCs. Hoxb5$^+$ HSCs and Hoxb5$^-$ HSCs were isolated from 2-year-old CD45.2
868 *Hoxb5*-tri-mCherry mice and were transplanted into lethally irradiated CD45.1 recipient
869 mice with 2×10^5 supporting cells (Hoxb5$^+$ HSCs, n = 13; Hoxb5$^-$ HSCs, n = 10). For
870 secondary transplants, 1×10^7 whole BM cells were transferred from primary recipient
871 mice. Abbreviations: PB = Peripheral blood, RT = Radiation therapy.
872 (C) Percentage chimerism at 16 weeks after receiving ten aged Hoxb5$^-$ HSCs or ten aged
873 Hoxb5$^+$ HSCs. Each column represents an individual mouse.
874 (D) Percentage chimerism at 16 weeks after whole BM secondary transplantation. Donor
875 whole BM cells for secondary transplantation were taken from mice denoted by * in
876 Figure 2C.
877 (E) Kinetics of average donor chimerism in each PB fraction after primary
878 transplantation.
879 (F) Kinetics of average donor chimerism after secondary transplantation.
880 (G) Kinetics of average donor myeloid output (myeloid proportion in donor cells) in LT-
881 HSC recipient mice after primary and secondary transplantation. *$P < 0.05$. **$P < 0.01$.
882 ***$P < 0.001$. Data and error bars represent means ± standard deviation.
883
884

885 **Figure 3.**

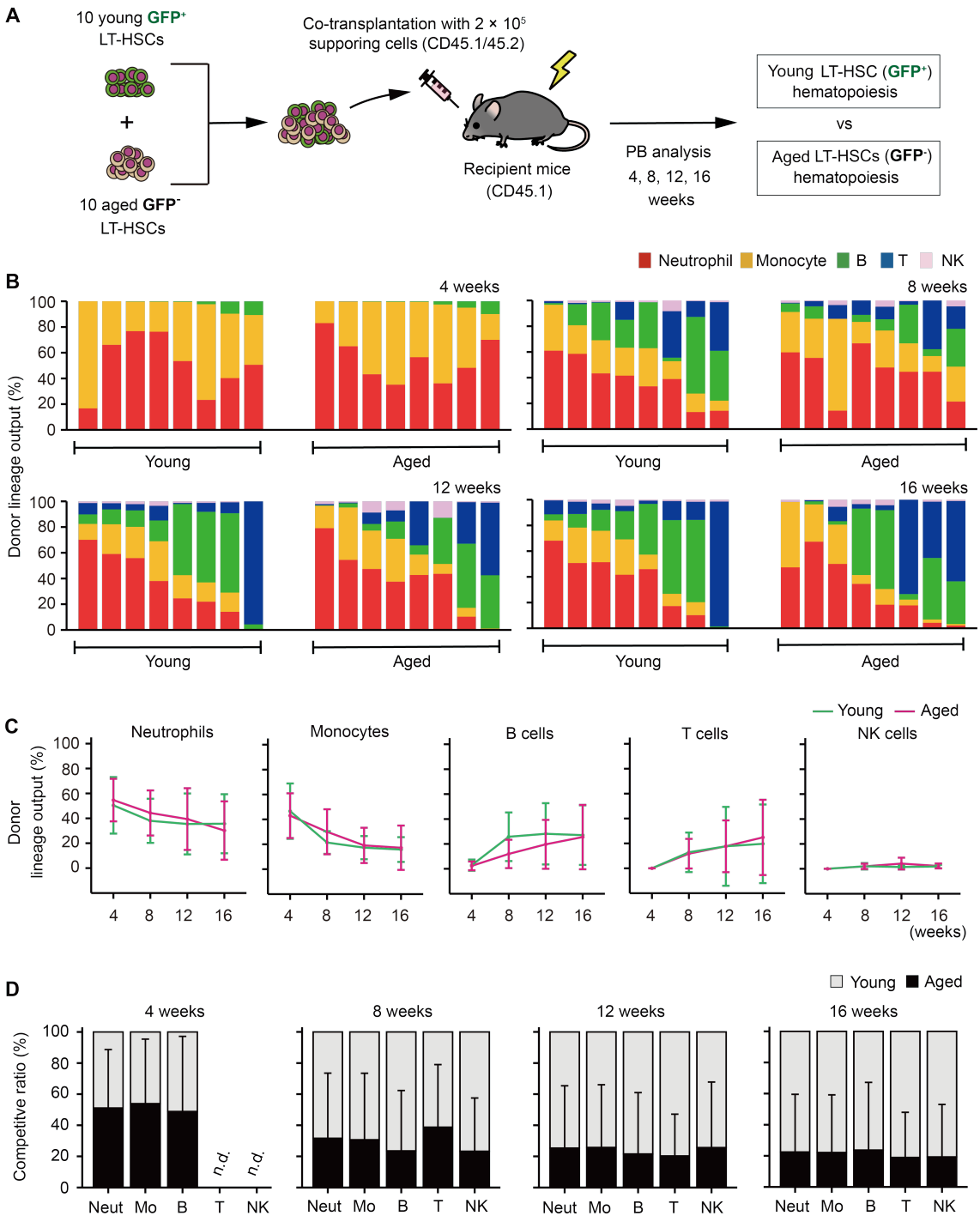

Figure 3. Aged LT-HSCs show balanced hematopoiesis throughout life

908 (A) Experimental design for competitive co-transplantation assay using young LT-HSCs
909 sorted from *Hoxb5*-tri-mCherry GFP mice and aged LT-HSCs sorted from *Hoxb5*-tri-
910 mCherry mice. Ten CD45.2^{+} young LT-HSCs and ten CD45.2^{+} aged LT-HSCs were
911 transplanted with 2×10^{5} CD45.1^{+}/CD45.2^{+} supporting cells into lethally irradiated
912 CD45.1^{+} recipient mice ($n = 8$).
913 (B) Lineage output of young or aged LT-HSCs at 4, 8, 12, 16 weeks after transplantation.
914 Each bar represents an individual mouse.
915 (C) Lineage output kinetics of young LT- HSCs or aged LT- HSCs at 4, 8, 12, 16 weeks
916 post-transplant.
917 (D) Competitive analysis of young LT-HSCs vs. aged LT-HSCs lineage output at 4, 8,
918 12, 16 weeks post-transplant. Competitive ratio was calculated as the proportion of young
919 LT-HSCs derived cells vs. aged LT- HSCs derived cells in each fraction. Abbreviations:
920 Neut = Neutrophils, Mo = Monocytes, B = B cells, T = T cells, and NK = NK cells. Data
921 and error bars represent means ± standard deviation. “n.d.” stands for “not detected.”
922
923
924
925
926
927
928
929
930
931

Figure 4.

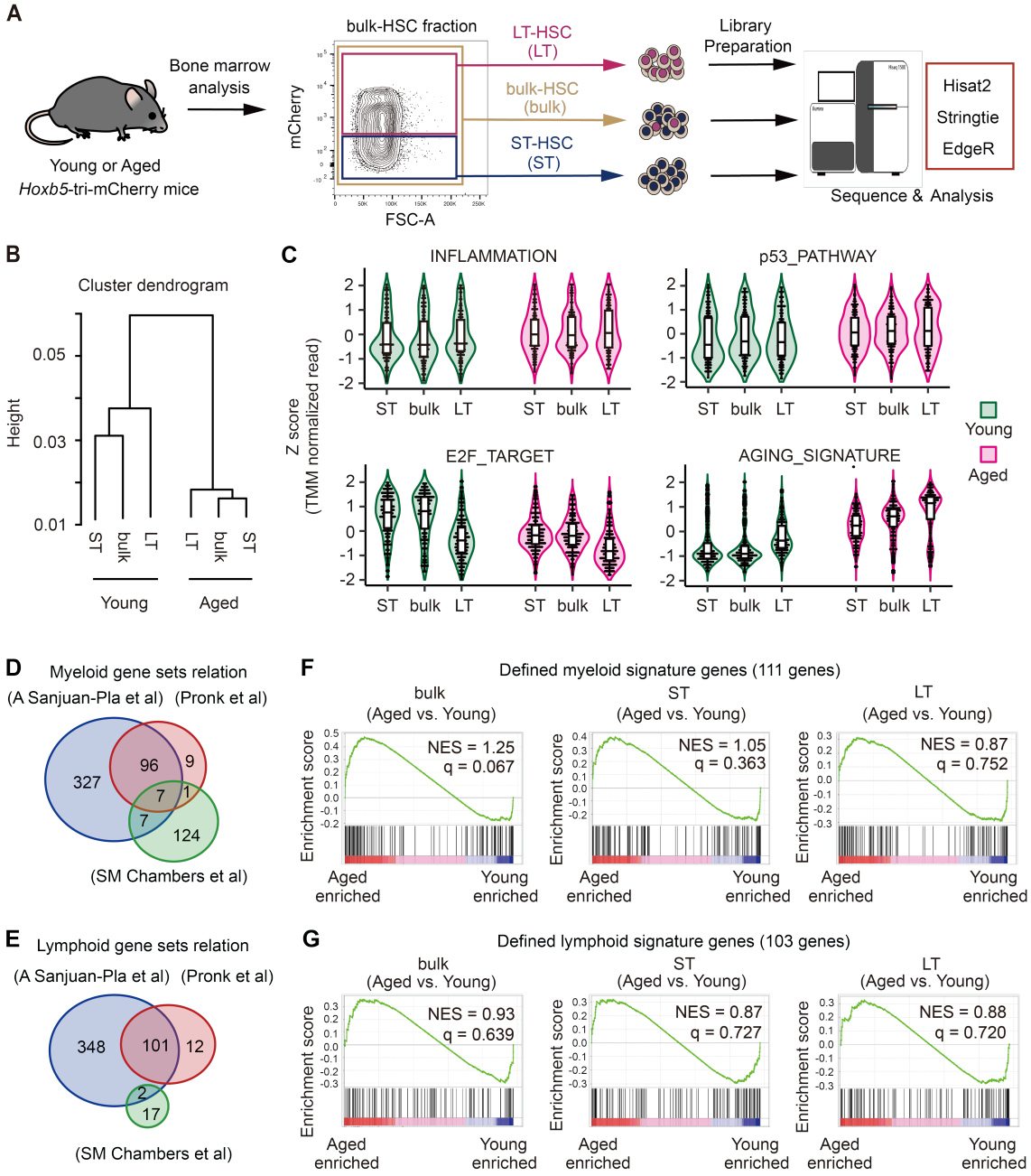

Figure 4. Myeloid-associated genes were not enriched in aged LT-HSCs compared to their young counterparts

954 (A) Experimental schematic for transcriptome analysis. LT-HSCs (n = 3), ST-HSCs (n =
955 3), and bulk-HSCs (n = 3) were sorted from young (2-3 months) or aged (23-25 months)
956 *Hoxb5*-tri-mCherry mice, after which each RNA was harvested for RNA sequencing.
957 (B) Hierarchical clustering dendrogram of whole transcriptomes using Spearman distance
958 and the Ward clustering algorithm.
959 (C) Violin plots showing normalized gene expression levels for each gene set in young
960 and aged LT-HSCs, ST-HSCs, and bulk-HSCs. Expression values for each gene were
961 standardized independently by applying *Z* score transformation.
962 (D, E) Venn diagram showing the overlap of genes between three myeloid signature gene
963 sets, and lymphoid signature gene sets (A Sanjuan-Pla et al., 2013, Pronk et al., 2007, SM
964 Chambers et al., 2007).
965 (F, G) Signature enrichment plots from GSEA analysis using defined myeloid and
966 lymphoid signature gene sets that overlapped in the three gene sets. Values indicated on
967 individual plots are the normalized Enrichment Score (NES) and q-value of enrichment.
968
969
970
971
972
973
974
975
976
977

Figure 5.

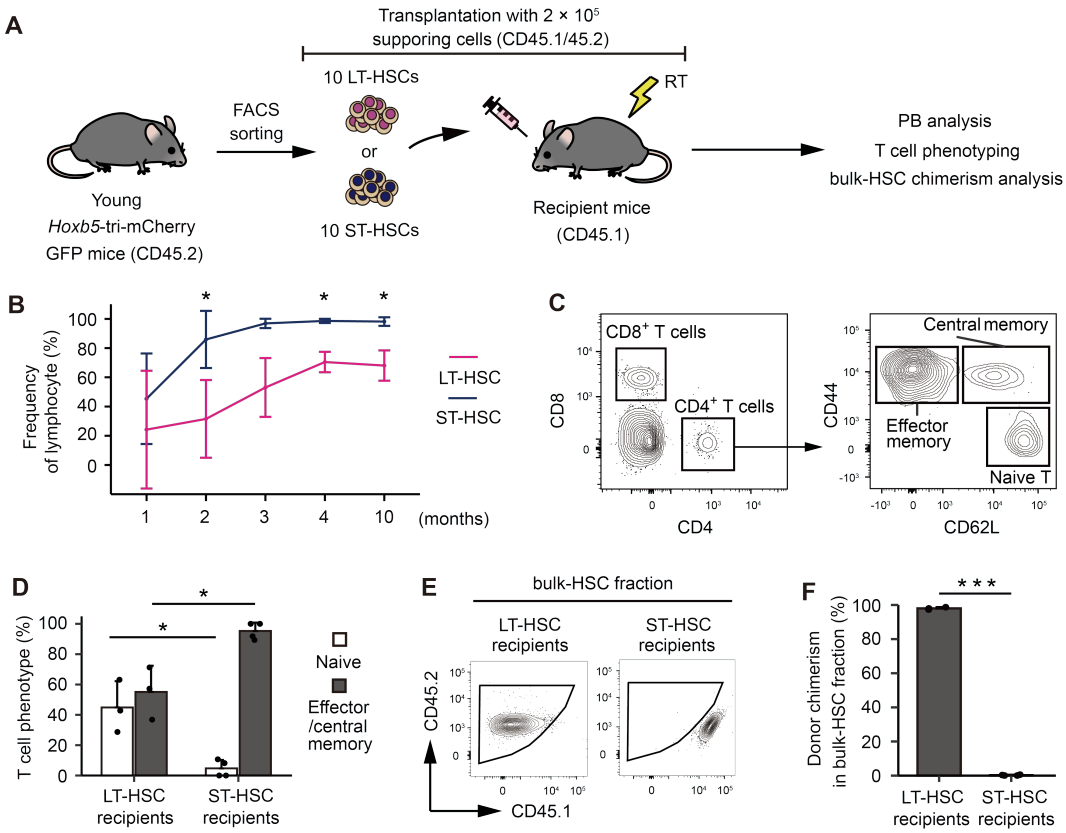

Figure 5. The memory-type lymphocytes in the peripheral blood make it look as if ST-HSCs are lymphoid-biased HSCs

(A) Experimental design for assessing the lineage output of young LT-HSCs or ST-HSCs. Ten LT-HSCs, or ten ST-HSCs were isolated from 2-month-old CD45.2 *Hoxb5*-tri-mCherry GFP mice and were transplanted into lethally irradiated CD45.1 recipient mice with 2×10^5 supporting cells (LT-HSCs, $n = 3$; ST-HSCs, $n = 4$).

(B) Kinetics of average frequency of lymphoid cells (B cells, T cells, and NK cells) in donor fraction after LT-HSCs or ST-HSCs transplantation.

(C) Gating scheme to identify memory (Central and effector) T cells and naive T cells in the PB after excluding doublets, dead cells, and non-donor cells.

1002 (D) Percentage of memory (Central and effector) T cells and naive T cells in donor $CD4^+$
1003 fraction 10 months after LT-HSC or ST-HSC transplantation.
1004 (E) Gating scheme to identify donor cells in bulk-HSC fraction in bone marrow analysis.
1005 (F) Donor chimerism in bulk-HSC fraction 12 months after LT-HSCs or ST-HSCs
1006 transplantation. *$P < 0.05$. ***$P < 0.001$. Data and error bars represent means ± standard
1007 deviation.
1008
1009
1010
1011
1012
1013
1014
1015
1016
1017
1018
1019
1020
1021
1022
1023
1024
1025

1026 **Figure 6.**

1027 1028 1029 1030 1031 1032 1033 1034 1035 1036 1037 1038 1039 1040 1041 1042 1043

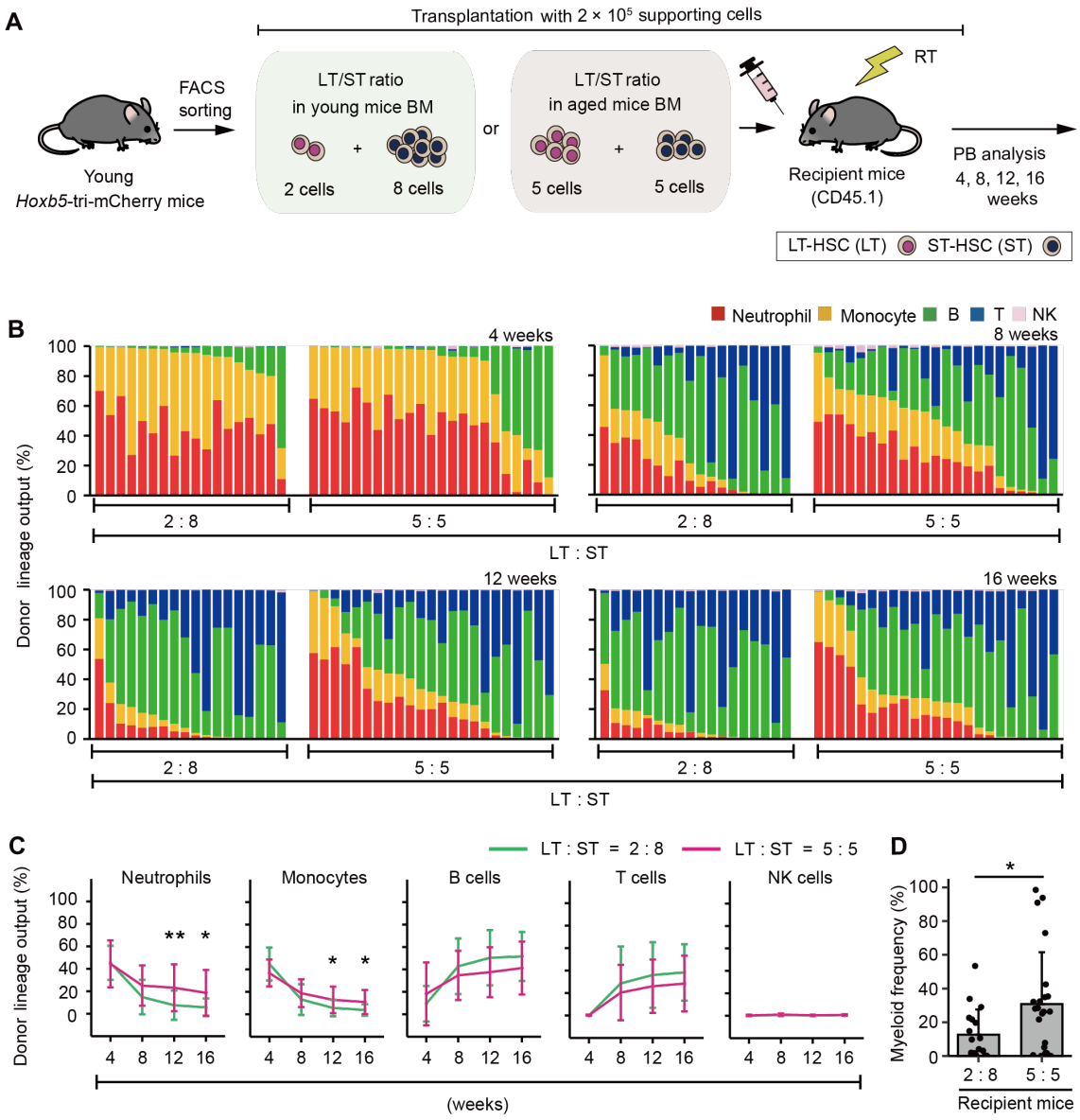

1044

1045 **Figure 6. Hematopoiesis after transplantation inclined either toward myeloid or**

1046 **lymphoid cell production by artificially changing the ratio of LT-HSC/ST-HSC**

1047 (A) Experimental design for the transplantation of 2-3-month-old LT-HSCs and ST-

1048 HSCs in a 2:8 ratio (the same ratio as in young mice BM) or 5:5 ratio (the same ratio as

1049 in aged mice BM). Donor cells were transplanted with 2 × 10^5 CD45.1$^+$/CD45.2$^+$

1050 supporting cells into lethally irradiated CD45.1^{+} recipient mice (2:8 ratio, n = 18; 5:5
1051 ratio, n = 23).
1052 (B) Donor lineage output of young LT-HSCs and ST-HSCs transplanted either in a 2:8
1053 ratio or a 5:5 ratio at 4, 8, 12, 16 weeks post-transplant. Each bar represents an individual
1054 mouse.
1055 (C) Kinetics of average lineage output of young LT-HSCs and ST-HSCs in a 2:8 ratio or
1056 a 5:5 ratio at 4, 8, 12, 16 weeks post-transplant.
1057 (D) Frequency of myeloid cells in donor cell fraction. *$P < 0.05$. **$P < 0.01$. Error bars
1058 represent standard deviation. Data represent two independent experiments.
1059
1060
1061
1062
1063
1064
1065
1066
1067
1068
1069
1070
1071
1072
1073

Figure 7.

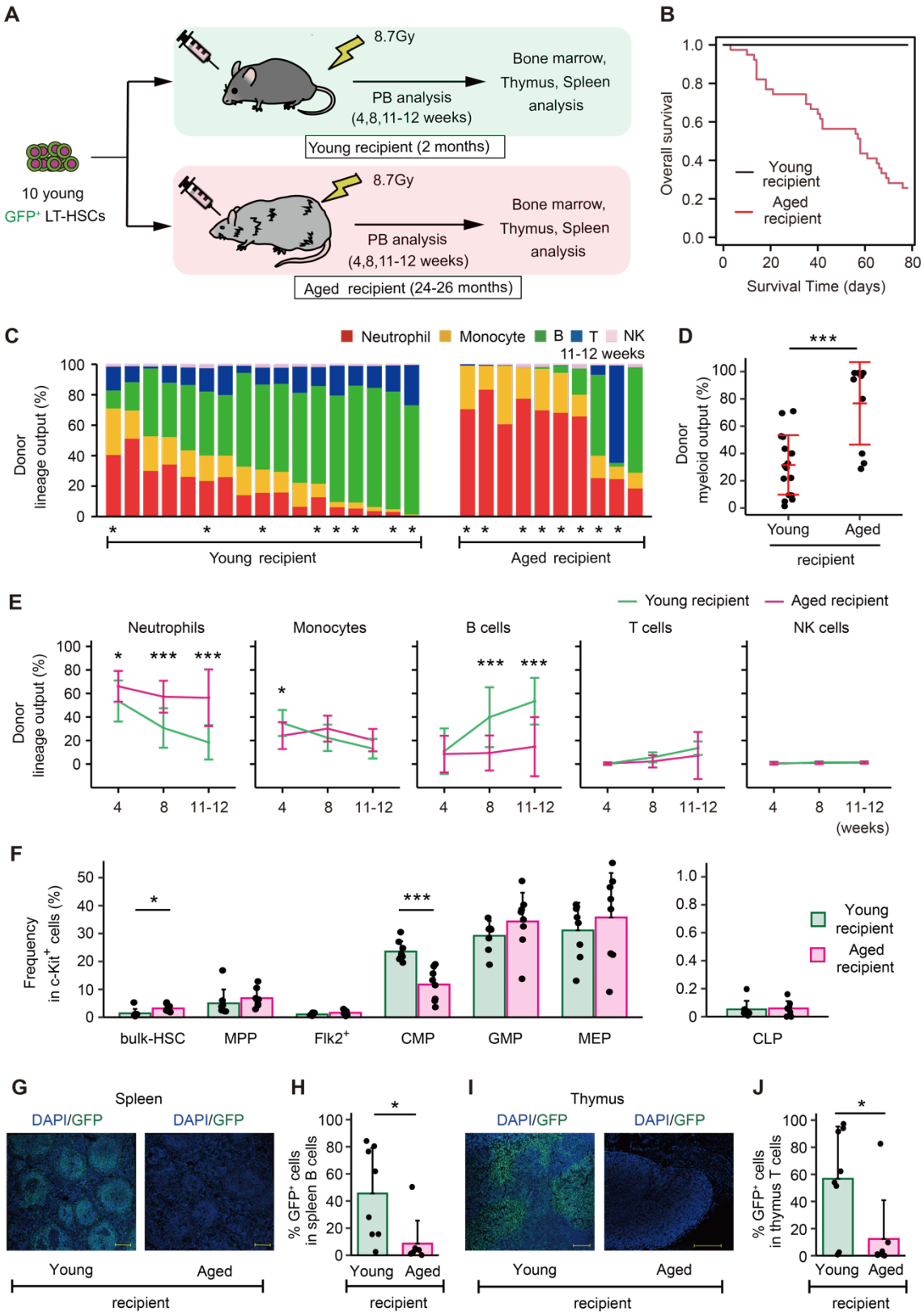
A
8.7Gy
Bone marrow, Thymus, Spleen analysis
PB analysis (4,8,11-12 weeks)
Young recipient (2 months)
10 young GFP+ LT-HSCs
8.7Gy
Bone marrow, Thymus, Spleen analysis
PB analysis (4,8,11-12 weeks)
Aged recipient (24-26 months)
B
Overall survival
Survival Time (days)
Young recipient
Aged recipient
C
Neutrophil Monocyte B T NK
11-12 weeks
Donor lineage output (%)
Young recipient
Aged recipient
D
Donor myeloid output (%)
Young
Aged
recipient
E
Young recipient
Aged recipient
Neutrophils
Monocytes
B cells
T cells
NK cells
Donor lineage output (%)
(weeks)
F
Frequency in c-Kit+ cells (%)
bulk-HSC
MPP
Flk2+
CMP
GMP
MEP
CLP
Young recipient
Aged recipient
G
Spleen
DAPI/GFP
DAPI/GFP
Young
Aged
recipient
H
% GFP+ cells in spleen B cells
Young
Aged
recipient
I
Thymus
DAPI/GFP
DAPI/GFP
Young
Aged
recipient
J
% GFP+ cells in thymus T cells
Young
Aged
recipient

1098 **Figure 7. Age-associated physiological changes drive differentiation of LT-HSCs**
1099 **toward myeloid cells**

1100 (A) Experimental design for assessing the impact of age-associated physiological changes
1101 on differentiation of LT-HSCs. Ten GFP^+ LT-HSCs sorted from young (2-3 months)
1102 *Hoxb5*-tri-mCherry GFP mice, were transplanted with 2×10^5 $CD45.1^+/CD45.2^+$
1103 supporting cells into lethally irradiated young or aged recipient mice. We defined donor
1104 cells as GFP^+ cells and supporting cells as $CD45.1^+/CD45.2^+$ cells.

1105 (B) Survival rate of recipient mice in each group.

1106 (C) Donor lineage output in young or aged recipient mice 11-12 weeks after transplanting
1107 young LT-HSCs (young recipient, $n = 17$; aged recipient, $n = 10$).

1108 (D) Myeloid output (Frequency of donor myeloid cells in donor fraction) in young or
1109 aged recipient mice 11-12 weeks after transplantation.

1110 (E) Kinetics of lineage output from donor LT-HSCs in young or aged recipient mice 4, 8,
1111 11-12 weeks after transplantation.

1112 (F) Average frequency of donor bulk-HSC and progenitor cells in donor c-Kit^+ cells in
1113 BM (young recipient, $n = 8$; aged recipient, $n = 8$). BM samples were taken from mice
1114 denoted by * in Figure 7C.

1115 (G) Representative immunofluorescence images of frozen spleen sections derived from
1116 young or aged recipient mice. Green: donor cells (GFP fluorescence); blue: DNA (DAPI);
1117 Scale bar: 200 μm.

1118 (H) Frequency of donor cells in spleen B cells of young or aged recipient mice (young
1119 recipient, $n = 8$; aged recipient, $n = 8$). Spleens are taken from mice denoted by * in Figure
1120 7C.

1121 (I) Representative immunofluorescence images of frozen thymus sections derived from
1122 young or aged recipient mice. Green: donor cells (GFP fluorescence); blue: DNA (DAPI);
1123 Scale bar: 200 μm.
1124 (J) Frequency of donor cells in thymus T cells of young or aged recipient mice (young
1125 recipient, $n = 8$; aged recipient, $n = 8$). Thymi are taken from mice denoted by * in Figure
1126 7C. *$P < 0.05$. ***$P < 0.001$. Error bars represent standard deviation. Data represent two
1127 independent experiments.
1128
1129
1130
1131
1132
1133
1134
1135
1136
1137
1138
1139
1140
1141
1142
1143
1144

1145 **Figure 8.**

1146 **Self-renewal heterogeneity model**

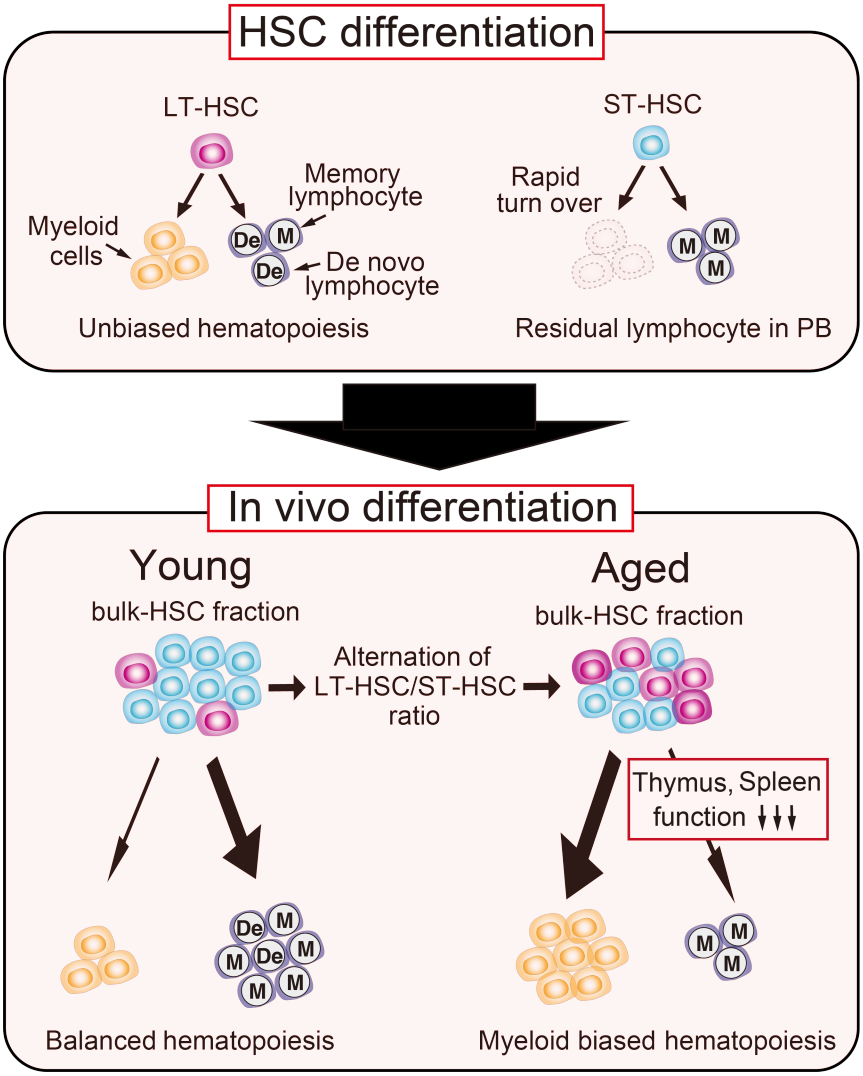

1147 1148 1149 1150 1151 1152 1153 1154 1155 1156 1157 1158 1159 1160 1161 1162

1163 **Figure 8.** Our new model: **Self-renewal heterogeneity model**. It has been thought that
1164 there were myeloid (My-) or lymphoid biased (Ly-) HSCs, and that clonal selection of
1165 My-HSCs caused age-associated myeloid biased hematopoiesis. However, in our model,
1166 LT-HSCs represent unbiased hematopoiesis throughout life. ST-HSCs lose their
1167 hematopoietic ability within a short period and memory-type lymphocytes remains in the
1168 PB after ST-HSC transplantation. These remaining memory-type lymphocytes make it

look as if ST-HSCs are lymphoid-biased (The upper section). As a result, the age-associated relative decrease of ST-HSCs in bulk-HSC fraction causes myeloid biased hematopoiesis with age. Additionally, the blockage of lymphoid differentiation at spleen and thymus accelerates further myeloid biased hematopoiesis in aged mice (The lower section).